Internet of Things 32 (2025) 101657

Contents lists available at ScienceDirect

Internet of Things

journal homepage: www.sciencedirect.com/journal/internet-of-things

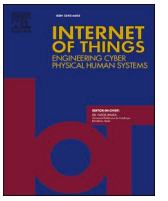

An energy-focused model for batteryless IoT: Vortex wireless power transfer and fog computing in 6 G networks

Mehdi Hosseinzadeh [a,b,1], Jawad Tanveer [c], Saqib Ali [d], Marcia L. Baptista [e], Farhad Soleimanian Gharehchopogh [f], Shakia Rajabi [f], Thantrira Porntaveetus [g,*], Sang-Woong Lee [h,*]

[a] School of Computer Science, Duy Tan University, Da Nang, Vietnam
[b] Jadara Research Center, Jadara University, Irbid 21110, Jordan
[c] Department of Computer Science and Engineering, Sejong University, Seoul 05006, Republic of Korea
[d] Department of Information Systems, College of Economics and Political Science, Sultan Qaboos University, Muscat 123, Oman
[e] NOVA Information Management School (NOVA IMS), Universidade Nova de Lisboa, Lisboa, 1070-312, Portugal
[f] Department of Computer Engineering, Ur., C., Islamic Azad University, Urmia, Iran
[g] Center of Excellence in Precision Medicine and Digital Health, Department of Physiology, Faculty of Dentistry, Chulalongkorn University, Bangkok, Thailand
[h] Pattern Recognition and Machine Learning Lab, School of Computing, Gachon University, Seongnam 13120, Republic of Korea

ARTICLE INFO

Keywords:
Batteryless IoT
Vortex wireless power transfer (WPT)
Fog computing
6 G
Quantum-inspired metaheuristic optimization

ABSTRACT

The Internet of Things (IoT) refers to the networked interconnection of devices that collect, exchange, and analyze data to enable intelligent applications. In emerging sixth-generation (6 G) networks, batteryless IoT devices have gained significant attention, as they rely on ambient energy harvesting rather than traditional batteries. This paper presents an energy-focused model for a 6G-enabled batteryless IoT network that integrates Vortex Wireless Power Transfer (WPT) with fog node coordination to manage energy harvesting and computation offloading. WPT exploits electromagnetic resonance to deliver energy wirelessly. Our vortex-based model applies exponential attenuation, enhancing energy harvesting for batteryless IoT devices. Then system dynamically assigns IoT devices to optimal WPT zones based on coverage and received power, while simultaneously determining whether tasks should be executed locally or offloaded to Mobile Edge Computing (MEC)-enabled fog nodes, based on real-time energy and latency constraints. To solve the result of the NP-hard optimization problem, we develop an Enhanced Adaptive Quantum Binary Particle Swarm Optimization (EAQBPSO) algorithm that effectively balances workload distribution, energy harvesting, and consumption. Simulation results indicate that our approach significantly outperform traditional methods, achieving improvements of up to 71 % in energy efficiency, nearly 87 % in energy harvesting efficiency, and reducing average energy consumption per task by over 40 %.

* Corresponding authors.
E-mail addresses: mehdihosseinzadeh@duytan.edu.vn (M. Hosseinzadeh), Jawadtanveer@sejong.ac.kr (J. Tanveer), saqib@squ.edu.om (S. Ali), m.baptista@novaims.unl.pt (M.L. Baptista), bonab.farhad@gmail.com (F.S. Gharehchopogh), shakiba.rajabi@ieee.org (S. Rajabi), thantrira.p@chula.ac.th (T. Porntaveetus), slee@gachon.ac.kr (S.-W. Lee).
[1] These authors contributed equally to this work.

https://doi.org/10.1016/j.iot.2025.101657

Available online 19 May 2025

1. Introduction

In the rapidly changing world of the Internet of Things (IoT), the growth of batteryless devices present challenges for keeping them working due to severe energy limits. Many of these devices rely on ambient energy harvesting rather than traditional batteries, making efficient energy management a key concern [1]. As IoT applications grow, especially in 6G-enabled networks where ultra-fast data rates and low latency are needed, the demand for new solutions becomes even more urgent [2,3]. 6 G networks are envisioned to operate at terahertz frequencies, enabling data rates over 1 Tbps, sub-millisecond latency, and real-time processing. They integrate edge intelligence, network slicing, and quantum-level security to support mission-critical applications and massive IoT deployments [4]. WPT emerges as a promising technology by enabling devices to harvest energy directly from dedicated sources, thus mitigating the reliance on limited onboard power supplies [5–7]. Unlike the traditional Radio Frequency (RF)-based WPT which suffer from high path loss and limited power delivery efficiency over distance, Vortex WPT uses structured electromagnetic waves to improve energy transfer [8]. The vortex-based method minimizes signal attenuation by using exponential attenuation models, letting devices harvest energy more efficiently at greater distance. Also, it's spatially selective power distribution lets targeted energy delivery, reducing interference and energy dissipation compared to RF-WPT [9].

Currently, fog computing offers a decentralized processing method and allowing for the offloading of computationally intensive tasks to near MEC servers [10–12]. MEC decentralizes processing by deploying compute resources at base stations or access points. It minimizes data travel to distant clouds, enabling ultra-low-latency services, better bandwidth usage, and localized AI inference in latency-critical scenarios like smart cities and connected vehicles [13,14]. This method not only reduce the energy burden on individual devices but also enhance overall system responsiveness and reliability [15]. Together, WPT and fog computing provide a robust framework that addressing the dual challenges of energy scarcity and computational limitations in batteryless IoT networks, which pave the way for more robust and sustainable deployments.

In this study, the primary challenge is to optimize the allocation of energy and computational tasks in a 6G-enabled IoT network by using WPT for energy harvesting and fog computing for task offloading, while simultaneously ensure low latency and high operational efficiency. Existing methods often fall short in maintain energy sustainability because they do not fully address the variability of ambient energy sources and fluctuate device power demands, based on the reports in [16,17]. Moreover, conventional approaches struggle with achieving balanced workload distribution and fairness among fog nodes, which lead to resource contention and degraded performance under different network conditions. Moreover, recent advances in secure task offloading [18] and RIS-assisted energy harvesting for IoT [19] highlight the importance of intelligent, decentralized optimization in dynamic, energy-constrained 6 G environments. This work aim to overcome these limitations by developing an adaptive optimization framework that integrate real-time energy status with intelligent offloading decisions, thereby improving overall system efficiency and ensuring equitable resource utilization across the network.

The proposed solution integrates Vortex WPT and fog computing within a 6G-enabled IoT network to address the energy constraints of batteryless devices. In our model, each IoT device dynamically select the optimal WPT zone based on real-time coverage and received power metrics, and maximizing energy usage. Simultaneously, the model coordinates computation offloading to near MEC-enabled fog nodes, and process tasks under latency and capacity constraints. This dual-layer method not only improves energy availability but also enhance workload balancing and system responsiveness across the network.

To tackle the NP-hard optimization challenge inherent in jointly managing WPT-based energy harvesting and computation

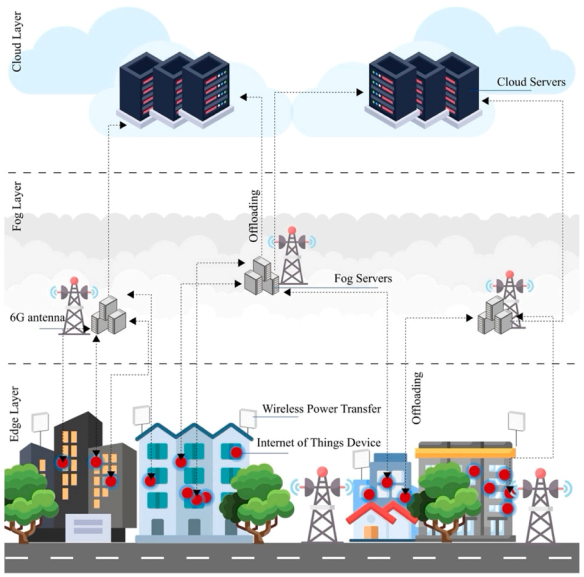

Fig. 1. 6G-Enabled Multi-Layer IoT Architecture Integrating Fog Coordination and Vortex WPT.

offloading, we introduce the EAQBPSO algorithm. EAQBPSO leverages a quantum-inspired representation that map continuous particle positions into binary decisions via a dynamic transfer function. It employs adaptive parameter tuning—including a linearly decreasing inertia weight and time-varying transfer function parameters—as well as swarm mean guidance to steer particles toward promising regions of the search space. These mechanisms enable EAQBPSO to efficiently optimize task scheduling and energy allocation, thereby significantly improving energy efficiency, sustainability, and resource fairness compared to conventional approaches. The main contributions of this study are:

- We propose a novel energy-focused model that integrates Vortex WPT with MEC-enabled fog computing, enabling batteryless IoT devices to dynamically harvest energy and offload computational tasks to sustain continuous operation in 6 G networks.
- We formulate a comprehensive, NP-hard optimization problem that jointly minimizes the net energy deficit while satisfying energy sustainability, latency, and fog capacity constraints.
- We develop and implement the EAQBPSO algorithm, which leverages quantum-inspired representations, adaptive parameter tuning, and swarm mean guidance to optimize task scheduling and energy management.

Fig. 1 illustrates a three-layer 6G-enabled architecture integrating Vortex WPT, fog computing, and cloud support for batteryless IoT devices. The edge layer comprises ambient-powered IoT sensors and 6 G antennas that handle local sensing and communication. These devices harvest energy wirelessly from nearby WPT units. Tasks are dynamically offloaded to nearby fog servers in the fog layer, enabling low-latency processing. For large-scale data handling or global optimization, tasks are further escalated to the cloud layer. This diagram visualizes how real-time coordination of power and computation is achieved across layers via 6 G connectivity.

The rest of the paper is structured as follows. Section 2 reviews related studies on energy harvesting batteryless IoT networks, highlighting gaps our work addresses. Section 3 presents our system model, integrating Vortex WPT with MEC-enabled fog nodes for dynamic computation offloading. Section 4 describes the simulation setup and experimental parameters. Section 5 discusses simulation results, performance metrics, and algorithmic comparisons. Finally, Section 6 concludes the paper and outlines future research directions.

2. Related studies

In recent years, significant research has focuse on addressing the energy limitations of batteryless IoT devices, particularly as these devices become important to emerging 6 G networks characterized by ultra-high data rates and low latency. Sabovic et al. [20] proposed energy-aware task scheduling for batteryless IoT devices by design a mechanism that dynamically adjusts execution based on task dependencies and voltage thresholds. Delgado et al. [21] further advance this field by formulating the scheduling problem as a Mixed Integer Linear Program that integrate energy prediction to address the on–off behavior typical of energy-harvesting systems, thereby provide important insights into managing constrained power environments. Additionally, Sabovic et al. [22] extended these concepts to support Tiny Machine Learning applications on batteryless devices by optimizing the decision between local inference and offloading to cloud services, thus effectively managing energy resources in real time.

Complementary to scheduling techniques, advancement in hardware design have also was critical. Yang et al. [23] proposed an energy harvesting circuit for batteryless IoT beacon tags that maximize power conversion efficiency through innovative techniques, such as charge pumping with shoot-through suppression and adaptive maximum power point tracking. Lacerda et al. [24] contributed by developing a behavioral model for RF-based WPT systems using supercapacitors, and provide a detailed analysis of charging and transmission cycles to optimizes energy storage and usage. On the computation offloading side, Tang et al. [25] introduced a grey wolf optimizer method to address task offloading in MEC systems with batteryless IoT, that allocating resources under intermittent operational condition. Wang et al. [26] designe a batteryless sensor chip for Agri-IoT that combine RF energy harvesting with event-driven data acquisition, significantly reduces energy consumption and extending device lifespan.

Furthermore, Bolourian et al. [27] proposed a three-tier wireless-powered mobile-edge computing framework integrate cloud computing, MEC, and IoT layers to jontly optimize WPT and computation offloading. Their framework employ combinatorial optimization and graph matching techniques to manage energy and computation resources effectively. In industrial settings, Van Leemput et al. [28] investigated strategies for integrate batteryless energy harvesting devices into multi-hop wireless sensor network, and address synchronization challenges cause by intermittent energy supply. Puluckul et al. [29] introduced TEGBed, a testbed for evaluating the efficiency of batteryless devices powered by thermal energy, enabling comprehensive, unsupervised assessment of power management strategies. Complementing these hardware and scheduling solutions, Fan et al. [30] developed a mathematical framework based on Martingale theory to analyze energy self-sustainability in RF-based WPT networks, providing a robust criterion for uninterrupted operation of batteryless devices.

Table 1 presents a comparative evaluation of existing approaches related to task scheduling, WPT integration, and offloading optimization in batteryless IoT systems. It highlights the core contributions and limitations of each study, demonstrating that prior work often addresses these aspects in isolation. In contrast, our proposed model uniquely integrates all three dimensions—task scheduling, energy harvesting via vortex-based WPT, and fog-assisted offloading—providing a holistic solution to the energy and computation challenges in 6G-enabled IoT networks.

Collectively, these studies demonstrate a multifaceted approach to overcoming the inherent energy constraints of batteryless IoT systems. However, traditional methods often struggle to integrate energy harvesting with dynamic computation offloading, particularly under the stringent conditions imposed by 6 G networks. To address this challenge, our proposed model integrates Vortex WPT with fog node coordination to dynamically manage energy harvesting and computation offloading in a 6G-enabled IoT network. The

Table 1
Characteristics of the related approaches and this study.

Study	Task Scheduling	WPT Integration	Offloading Optimization	Main Contributions	Limitations
[20]	✓	×	×	Task scheduling under energy constraints	Limited adaptability to real-time changes
[21]	✓	×	×	Mixed Integer Linear Program for task execution	Assumes idealized energy prediction model
[22]	✓	×	✓	Energy-aware TinyML inference decision-making	Focuses only on inference, not broader IoT tasks
[23]	×	✓	×	High-efficiency energy harvesting circuit	Lacks integration with MEC for computation
[24]	×	✓	×	Behavioral modeling of RF-WPT supercapacitor	Does not address computational optimization
[25]	✓	×	✓	Discrete GWO for MEC offloading	Limited performance under highly dynamic conditions
[26]	×	✓	×	RF energy-harvesting chip for Agri-IoT	Designed for agriculture, not general IoT
[27]	✓	✓	✓	Three-tier MEC-WPT optimization framework	High complexity in large-scale deployments
[28]	×	×	×	Strategies for batteryless multi-hop networks	Challenges in network synchronization
[29]	×	×	×	Thermal energy-based testbed for batteryless IoT	Limited evaluation for diverse energy sources
[30]	×	✓	×	Martingale-based self-sustainability analysis	Does not integrate real-time energy adaptation
Our Study	✓	✓	✓	Vortex WPT and MEC fog-based offloading	Computational overhead in highly dynamic networks

model assigns each IoT device to the optimal WPT zone based on received power and coverage, and it makes real-time decisions on whether to process tasks locally or offload them to MEC-enabled fog nodes based on energy availability, processing requirements, and latency constraints.

The next section details our system model, encompassing task execution processes, resource limitations, and optimization goals.

3. System model

In this section, we describe the system model that underpin our proposed approach, focuses on the key components that influence task execution, energy usage, and computation offloading. our framework is integrate vortex WPT, fog computing, and MEC-enabled optimization to ensure efficient task allocation for batteryless IoT devices in a 6 G environment

Table 2 summarizes the key symbols and notations used throughout the system model and optimization formulation.

3.1. Network architecture

We consider a 6G-enabled IoT network consisting of N batteryless IoT devices, each capable of Vortex WPT reception, and a set of M Fog Nodes (MEC servers) responsible for both power coordination and computation offloading. Fig. 2 depicts three-dimensional schematic of dynamic WPT zone allocation for batteryless IoT devices in a proposed environment. IoT devices, represented by various smart appliances, are distributed across the XY plane and harvest energy from the nearest vortex-based WPT emitters located above. Each emitter creates a coverage region based on power attenuation, shown as concentric contours. Devices dynamically switch among these WPT zones to optimize energy reception. Red arrows indicate energy transfer paths. Communication between devices and fog nodes occurs via ultra-reliable, low-latency 6 G wireless links, enabling synchronized data offloading and energy coordination in real time.

Formally, let $\mathscr{D} = \{1, 2, \ldots, N\}$ be the set of IoT devices, $\mathscr{Z} = \{1, 2, \ldots, Z\}$ be the set of Vortex WPT zones, and $\mathscr{F} = \{1, 2, \ldots, M\}$ be the set of fog nodes.

Each IoT device $d \in \mathscr{D}$ must periodically perform sensing and (optionally) offload computation to one of the fog nodes in $\mathscr{F}$. The power management and zone assignment decisions are made in near real-time to maintain sufficient energy levels and meet latency constraints.

3.1.1. IoT devices

Each IoT device d is batteryless, meaning it rely on harvested energy to power its operations. Define $P_d(d)$ as power demand for device d to complete one sensing-and-transmission cycle, and $P_{\text{th}}(d)$ as threshold power below which device d cannot operates (i.e., it

Table 2
Applied abbreviations in the study.

Symbols	Description	Symbols	Description
$\mathscr{D}$	Set of batteryless IoT devices	$\mathscr{F}$	Set of fog nodes
$\mathscr{Z}$	Set of vortex WPT zones	D	Index for IoT device
I	Index for WPT zone	f	Index for fog node
T	Discrete time slot	$x_d(t)$	Position of device dd at time t
$P_d(d,t)$	Power demand of device d at time t	α_d	Baseline power demand of device d
β_d	Power fluctuation factor of device d	ω	Frequency of power fluctuation
$P_{\text{th}}(d)$	Power threshold below which device d cannot operate	$P_{\text{wpt},i}$	Nominal transmitted power by WPT zone i
η_i	Transmission efficiency of WPT zone i	$r_{d,i}$	Distance from device d to center of zone i
c_i	Center coordinate of WPT zone i	R_i	Maximum coverage radius of WPT zone i
Λ	Vortex attenuation coefficient	$x_{d,i}(t)$	Binary variable: 1 if device d assigned to zone i at time t
$y_{d,f}(t)$	Binary variable: 1 if device d offloads to fog node f at time t	C_f	Processing capacity of fog node f
E_f	Energy consumed by fog node f per offloaded task	τ_f	Latency constraint at fog node f
$\tau_{\text{offload}}(d,f,t)$	Offloading delay from device d to node f at time t	$E_{\text{net}}(d,t)$	Net energy balance of device d at time t
$E_{\text{recv}}(d,i)$	Harvested energy from zone i by device d	$E_{\text{cons}}(d)$	Energy consumption by device d
P_{tx}	Transmission power of device	T_{op}	Duration of sensing/processing phase
T_{tx}	Duration of transmission	$PL(d)$	Path loss in dB at distance d
PL_0	Path loss at reference distance	γ	Path loss exponent
X	Shadowing (random) factor	$P_{\text{rx}}(d)$	Received power at device d
P_{min}	Minimum required received power for offloading	O_d	Offloading decision indicator for device d
L_f	Current load on fog node f	L_{max}	Maximum allowed fog node load
M_d	Sustainability margin of device d	SM	Network-wide sustainability margin
DSR	Device Sustainability Ratio	FNUR	Fog Node Utilization Ratio
RAF	Resource Allocation Fairness	L_d	Offloaded load from device d
T	Number of epochs (in optimization)	$v_{i,j}(t)$	Velocity of particle i in dimension j at time t
$x_{i,j}(t)$	Position of particle i in dimension j at time t	$pbest_{i,j}$	Personal best of particle i
$gbest_j$	Global best of swarm in dimension j	$m_j(t)$	Swarm mean in dimension j
w(t)	Inertia weight at time t	$\lambda(t)$	Transfer function slope (adaptive)
$\delta(t)$	Transfer function threshold shift	$T(v)$	Transfer function (sigmoid)
N	Total number of particles	n	Dimension of solution space

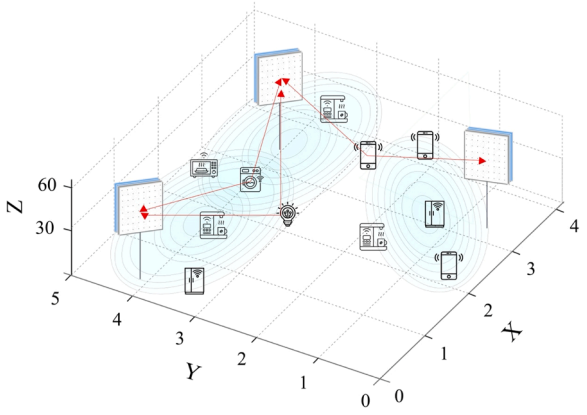

Fig. 2. 3D depiction with vortex-based WPT emitters above IoT devices, concentric coverage contours of power zones, dynamic switching via 6 G coordination.

fails to activate or complete a task).

We assume each device operates in discrete time slots $t = 1, 2, \ldots$ .At the start of time slot t, device d harvest energy from one Vortex WPT zone (if it is within coverage). If the harvested energy is insufficient ($P_{\text{recv}}(d,t) < P_d(d)$), the device either goes to sleep mode or attempts to offload if the fog node can supply additional power (e.g., through local wireless power bursts or an alternative WPT channel).

We define the instantaneous power demand of device d at time slot t as shown in Eq (1):

$$P_d(d,t) = \alpha_d\,(1+\beta_d \sin(\omega t)) \tag{1}$$

where α_d is the baseline power needed for sensing/transmission, β_d is a fluctuation factor (e.g., due to variable workload), and ω is the frequency of the load fluctuation.

3.1.2. Vortex WPT zones

We consider Z Vortex WPT zones, each characterized by Transmission Efficiency η_i (fraction of power that can be received), Center Position c_i in the deployment space, Maximum Coverage Radius R_i, beyond which the WPT signal is negligible.

Let $P_{\text{wpt},i}$ be the nominal power emitted by Vortex WPT zone i. The received power at device d from zone i at time t depends on the distance $r_{d,i}$ and any path-loss or vortex attenuation factors. A simplified expression is given by Eq (2):

$$P_{\text{recv}}(d,i,t) = \eta_i P_{\text{wpt},i} \exp\left(-\lambda r_{d,i}\right) \tag{2}$$

where λ is a vortex attenuation coefficient, and $r_{d,i} = ||c_i - x_d(t)||$ is the Euclidean distance between device d's position $x_d(t)$ and the center c_i of zone i. We assume each device is associated with exactly one WPT zone at a time slot t.

A device d can only be served by zone i if $r_{d,i} \le R_i$. Hence, we define a binary assignment $x_{d,i}(t)$, as shown by Eq (3):

$$\mathrm{x_{d,i}(t)} = \begin{cases} 1, & \textit{if } r_{d,i} \le R_i \textit{ and device } d \textit{ is assigned to zone } i \textit{ at time } t, \\ 0, & \textit{otherwise}. \end{cases} \tag{3}$$

3.1.3. Fog nodes and MEC

Each fog node $f \in \mathcal{F}$ has Processing Capacity C_f(e.g., CPU cycles per second), Energy Consumption per task E_f, and a latency constraint τ_f that must be met when tasks are offloaded.

When an IoT device d cannot gather enough power to locally complete its task, it may offload computation to a fog node f, provided that f has sufficient capacity available at time t. Defined as Eq (4):

$$\mathrm{y_{d,f}(t)} = \begin{cases} 1, & \textit{if device } d \textit{ offloads its task to fog node } f \textit{ at time } t, \\ 0, & \textit{otherwise}. \end{cases} \tag{4}$$

The fog node jointly decide which WPT zone the device should connect to and whether the device should offload. The MEC must ensure the device's harvested power meets or exceeds its threshold $P_{\text{recv}}(d,i,t) \ge P_{\text{th}}(d)$, and offloading is only performed if local energy is insufficient $P_{\text{recv}}(d,i,t) < P_d(d,t)$ or to meet latency constraints.

To capture the energy feasibility of each device and the offloading decision in a single framework, we defined the net energy of device d at time t as Eq (5):

$$E_{\text{net}}(d,t) = \sum_{i \in \mathcal{Z}} x_{d,i}(t)\, P_{\text{recv}}(d,i,t) - P_d(d,t)\left(1 - y_{d,f}(t)\right) - E_f\, y_{d,f}(t) \tag{5}$$

Where The second term $P_d(d,t)\left(1-y_{d,f}(t)\right)$ is the local energy consumption if the device does not offload ($y_{d,f}(t)=0$). The third term $E_f\, y_{d,f}(t)$ is the offloading energy overhead at the fog node if $y_{d,f}(t)=1$.

A feasibility constraint for each device d is given by Eq (6):

$$E_{\text{net}}(d,t) \geq 0, \quad \forall\, d \in \mathscr{D}, \forall\, t \tag{6}$$

We aim to maximize the total harvested energy while minimizing the overall system's energy shortfall and fog overhead. The objective is expressed as Eq (7):

$$\max_{\{x_{d,i}(t),\, y_{d,f}(t)\}} \left\{ \sum_{t=1}^{T} \sum_{d=1}^{N} E_{\text{net}}(d,t) \right\} \text{ subject to : } \begin{array}{c} x_{d,i}(t) \in \{0,1\} \\ y_{d,f}(t) \in \{0,1\} \\ \sum_{i \in \mathscr{Z}} x_{d,i}(t) \leq 1 \end{array} \quad \begin{array}{c} \sum_{f \in \mathscr{F}} y_{d,f}(t) \leq 1 \\ \text{Coverage Constraint : } r_{d,i} \leq R_i \Rightarrow x_{d,i}(t) = 1 \\ \text{Fog Capacity : } \sum_{d} y_{d,f}(t)\, P_d(d,t) \leq C_f \end{array} \tag{7}$$

$$\text{Latency : } \tau_f \geq \tau_{\text{offload}}(d,f,t)$$

Here, $\tau_{\text{offload}}(d,f,t)$ is the time needed to offload device d's task to node f. The binary constraints ensure a device is assigned to exactly one WPT zone per time slot and offloads to at most one fog node. The coverage constraint ensures assignment is possible only if the device is within range of the vortex zone. The fog capacity constraint ensures the total tasks offloaded to f do not exceed C_f.

To solve Eq (7), we form a Lagrangian $\mathscr{L}$ incorporating these constraints. For instance, let $\mu_f \geq 0$ be the Lagrange multiplier associated with fog capacity, $\lambda_{d,i}$ with coverage constraints, and so forth. Then, the Lagrangian function is formulated as Eq. (8).

$$\mathscr{L} = \sum_{t=1}^{T} \sum_{d=1}^{N} E_{\text{net}}(d,t) - \sum_{f=1}^{M} \mu_f \left(\sum_{d} y_{d,f}(t)\, P_d(d,t) - C_f \right) - \sum_{(d,i) \in \mathscr{D} \times \mathscr{Z}} \lambda_{d,i}\, \Psi_{d,i}(t) - \cdots \tag{8}$$

where $\Psi_{d,i}(t)$ encapsulates the coverage constraint $\left(r_{d,i} \leq R_i\right)$. By taking partial derivatives of $\mathscr{L}$ w.r.t. each decision variable $x_{d,i}(t)$ and $y_{d,f}(t)$, we obtain Karush-Kuhn-Tucker (KKT) conditions that yield the optimal zone assignment and offloading strategy, as expressed in Eq. (9):

$$\frac{\partial \mathscr{L}}{\partial x_{d,i}(t)} = 0, \quad \frac{\partial \mathscr{L}}{\partial y_{d,f}(t)} = 0, \quad \mu_f, \lambda_{d,i} \geq 0, \quad \mu_f \left(\sum_{d} y_{d,f}(t)\, P_d(d,t) - C_f \right) = 0, \quad \ldots \tag{9}$$

Fig. 3 shows the decision process for dynamic energy harvesting and task offloading in a vortex-based WPT-enabled batteryless IoT network. IoT devices (IoT₁, IoT₂, IoT₃) dynamically associate with the nearest WPT zone. When the received power exceeds the device threshold, tasks are computed locally. Otherwise, when $P_{\text{recv}}(d,i,t) < P_d(d,t)$, the task is offloaded to a nearby MEC fog node. This mechanism ensures devices remain operational under energy constraints while maintaining latency and quality-of-service requirements through intelligent offloading and energy-aware task allocation.

3.2. Energy harvesting and consumption model

We assume each IoT device d harvests energy from a Vortex WPT zone $i \in \mathscr{Z}$ within its coverage range. The received energy

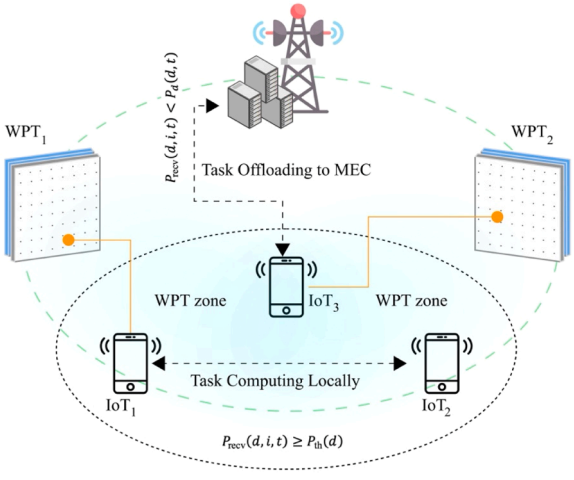

Fig. 3. Schematic of IoT devices in vortex WPT zones: compute locally when power threshold met, otherwise offload tasks to MEC nodes.

$E_{\text{recv}}(d,i)$ from zone i is expressed as Eq. (10):

$$E_{\text{recv}}(d,i) = \eta_i P_{\text{wpt}} e^{-\frac{d_i}{d_0}} \tag{10}$$

Where $\eta_i \in [0,1]$ is the WPT efficiency for zone i, P_{wpt} is the transmitted power by the Vortex WPT emitter, $d_i = |x_d - c_i|$ is the distance between device d (at position x_d) and the center of vortex i (at c_i), d_0 is a reference distance that normalizes the exponential attenuation factor.

The exponential term $e^{-\frac{d_i}{d_0}}$ models vortex attenuation over distance, ensuring that devices closer to the center receive more power. For computational simplicity, P_{wpt} may be assumed constant or adjusted dynamically by the MEC node to meet network-level energy constraints.

Each IoT device d requires energy to perform data sensing, processing, and transmission during a single operation cycle. Denote this total consumption by $E_{\text{cons}}(d)$, as calculated in Eq. (11):

$$E_{\text{cons}}(d) = P_d T_{\text{op}} + P_{\text{tx}} T_{\text{tx}} \tag{11}$$

Where P_d is the power demand of device d for local sensing/processing, T_{op} is the operation time for the sensing/processing phase, P_{tx} is the transmission power used by device d to send data, T_{tx} is the transmission duration.

Depending on the traffic load or quality of service requirements, P_d and P_{tx} may vary over time, e.g., $P_d(t)$ and $P_{\text{tx}}(t)$. In such cases, $E_{\text{cons}}(d)$ becomes time-dependent, but we omit the explicit time index here for clarity.

A device d is considered energy-deficient if the harvested energy at any cycle is strictly less than the required consumption, as shown in Eq. (12):

$$E_{\text{recv}}(d,i) < E_{\text{cons}}(d) \tag{12}$$

When inequality Eq. (12) is met, device d cannot complete its operation unless it switches to a more suitable WPT zone or receives an additional power boost from the fog node. This situation triggers Dynamic WPT Zone Switching, where the MEC-based controller reassigns device d to a different zone $j \neq i$ that may offer higher power reception (subject to coverage constraints and system-level optimization).

By integrating these equations into the overall system model (Section 3.1) and the subsequent optimization framework (Section 4), we ensure that devices can seamlessly transition between vortex zones to maintain energy sufficiency and continuous operation in a 6 G IoT environment.

3.3. Wireless communication model

Each IoT device $d \in \mathscr{D}$ communicates with a fog node $f \in \mathscr{F}$ via 6 G millimeter wave (mmWave) or Terahertz (THz) bands, achieving ultra-high data rates and low latency. Let P_{tx} be the transmission power used by the device, which may vary with time or application demands.

To account for propagation effects, we adopt a log-distance path loss model with additional shadowing. The path loss $PL(d)$ in dB at distance d from the transmitter is given by Eq. (13):

$$PL(d) = PL_0 + 10\gamma \log_{10}(d) + \chi \tag{13}$$

Where PL_0 is the reference path loss (in dB) at a certain reference distance (e.g., 1 m), γ is the path loss exponent, capturing how signal attenuation scales with distance, and χ is a shadowing term (in dB) that accounts for random variations due to obstacles, fading, or other environmental factors.

In a non-dB form, if P_{tx} is expressed in mW (or Watts), we write $P_{\text{rx}}(d) = \frac{P_{\text{tx}}}{10^{\frac{PL(d)}{10}}}$, thus linking the transmitted power to the received power after path loss.

A device d decides to offload its computation to a fog node f when local energy is insufficient $(E_{\text{recv}}(d) < E_{\text{cons}}(d))$, fog load L_f is below a maximum threshold L_{max}, and link quality (influenced by path loss) is adequate for offloading to succeed within the latency constraints.

To unify these conditions into one decision rule, let O_d be an offloading indicator, as expressed in Eq. (14):

$$\mathrm{O_d} = \begin{cases} 1, \ \textit{if} \ (E_{\text{recv}}(d) < E_{\text{cons}}(d)) \ \wedge \ \left(L_f < L_{max}\right) \ \wedge \ \left[P_{\text{tx}} - \left(PL_0 + 10\gamma \log_{10}(d) + \chi\right) \geq P_{min}\right], \\ 0, \ \textit{otherwise}. \end{cases} \tag{14}$$

Herem$E_{\text{recv}}(d)$ and $E_{\text{cons}}(d)$ come from Eq. (10) and Eq. (11) in Section 3.2 (Energy Harvesting & Consumption). L_f is the current load on fog node f, and L_{max} the maximum allowable load to guarantee latency. The term $\left[P_{\text{tx}} - \left(PL_0 + 10\gamma \log_{10}(d) + \chi\right) \geq P_{min}\right]$ ensures the received power (in dB scale) meets a minimum power requirement P_{min}r successful offloading.

In other words, $O_d = 1$ precisely when the device lacks sufficient local energy ($E_{\text{recv}} < E_{\text{cons}}$), the fog node can handle the extra task $\left(L_f < L_{max}\right)$, and the transmission link is strong enough $(P_{\text{rx}}(d) \geq P_{min})$.

By combining path loss Eq. (13), energy feasibility, and fog load constraints into Eq. (14), we obtain a single unified condition for computation offloading in our network.

3.4. Problem formulation

Our goal is to minimize the total net energy deficit across all IoT devices while ensuring system sustainability and managing MEC fog node capacity. In other words, we aim to reduce the gap between energy consumption and harvested energy through optimal WPT zone assignment and offloading decisions.

Zone Assignment: Define the binary variable, as given by Eq. (15):

$$x_{i,j} = \begin{cases} 1, & \textit{if IoT device } i \textit{ is assigned to WPT zone } j, \\ 0, & \textit{otherwise}. \end{cases} \tag{15}$$

Each device can be associated with at most one WPT zone at each decision epoch, as shown in Eq. (16):

$$\sum_{j \in \mathcal{Z}} x_{i,j} \leq 1, \quad \forall i \in \mathcal{D} \tag{16}$$

Offloading Decision: Define the binary indicator, as expressed in Eq. (17)

$$O_d = \begin{cases} 1, & \textit{if IoT device } d \textit{ offloads its computation to a MEC node}, \\ 0, & \textit{otherwise}. \end{cases} \tag{17}$$

The system must satisfy the following constraints:

Energy Sustainability: Each IoT device must harvest energy that is at least equal to its consumption in order to remain operational, as defined in Eq. (18):

$$E_{\text{recv},i} \geq E_{\text{cons},i}, \quad \forall i \in \mathcal{D} \tag{18}$$

where $E_{\text{recv},i}$ and $E_{\text{cons},i}$ are defined as in Sections 3.2.1 and 3.2.2, respectively.

MEC Fog Node Capacity: The total offloaded tasks must not exceed the maximum computation load L_{max} vailable at the MEC, as given by Eq. (19):

$$\sum_{i \in \mathcal{D}} O_d \leq L_{max} \tag{19}$$

Limited Zone Switching: To prevent excessive overhead in dynamic zone assignment, only a limited number of devices are allowed to switch WPT zones at any time step (embedded in constraint Eq. (16)).

The overall optimization problem can now be written as Eq. (20).

$$\begin{aligned} &\min_{\{x_{i,j},\, O_d\}} \sum_{i \in \mathcal{D}} \left(E_{\text{cons},i} - E_{\text{recv},i}\right) \\ &\text{s.t. } E_{\text{recv},i} \geq E_{\text{cons},i}, \ \forall i \in \mathcal{D} \\ &\sum_{j \in \mathcal{Z}} x_{i,j} \leq 1, \ \forall i \in \mathcal{D} \\ &\sum_{i \in \mathcal{D}} O_d \leq L_{max}, \\ &x_{i,j} \in \{0,1\}, \quad \forall i \in \mathcal{D}, \quad j \in \mathcal{Z} \\ &O_d \in \{0,1\}, \quad \forall d \in \mathcal{D}. \end{aligned} \tag{20}$$

In this formulation the objective function Eq. (20) minimizes the aggregated energy deficit, $E_{\text{cons},i} - E_{\text{recv},i}$, over all devices, constraint Eq. (18) guarantees that each device's harvested energy meets or exceeds its consumption, constraint Eq. (16) ensures that an IoT device is assigned to at most one WPT zone, constraint Eq. (19) keeps the total offloading load within the capacity limit of the MEC fog nodes, the binary nature $jx_{i,j}$ and O_d enforces discrete decision-making, making the problem NP-hard and well-suited to be addressed via hybrid metaheuristic algorithms.

3.5. Solution approach: enhanced adaptive quantum binary particle swarm optimization (EAQBPSO)

Our proposed algorithm, EAQBPSO, is designed specifically for the complex, combinatorial nature of energy and resource allocation in our 6G-enabled IoT network. It is a quantum-inspired hybrid that builds upon classical PSO but incorporates several key modifications to effectively handle binary decision variables and the highly nonconvex search space of our problem.

The original AQBPSO is a variant of Particle Swarm Optimization specifically designed for binary optimization problems. Its key features include:

Quantum-Inspired Representation: Rather than working directly with binary values, particles are represente in a continuous space (usually in $[0,1]^n$) and then mappe to binary decisions via a transfer (sigmoid) function. This probabilistic mapping is inspired by

quantum computing concepts such as superposition, which allows each particle to have a probability of being in the "0″ or "1" state.

Fixed Transfer Function: In the original formulation, the conversion from continuous particle positions to binary decisions is handled by a fixed sigmoid function, as expreesed by Eq. (21):

$$T(v) = \frac{1}{1 + \exp(-v)} \tag{21}$$

which is applied uniformly across all iterations.

The algorithm uses the classic PSO velocity update rule, as calculated in Eq. (22):

$$v_{ij}(t+1) = wv_{ij}(t) + c_1 r_1 \left(pbest_{ij} - x_{ij}(t)\right) + c_2 r_2 \left(gbest_j - x_{ij}(t)\right) \tag{22}$$

where the parameters (inertia weight w, and acceleration coefficients c_1, c_2) are typically fixed or follow a simple schedule.

Algorithm 1
Enhanced Adaptive Quantum Binary Particle Swarm Optimization (EAQBPSO).

Input:	Problem, population size N, epochs T, learning coefficient c3, parameters: w0, w_{min}, lambda0, lambda_min, delta0, delta_max
	Begin:
1	Initialization:
2	FOR i = 1 TO N DO:
3	Randomly initialize position$[i] \in [0,1]^n$
4	Randomly initialize velocity$[i] \in [-1,1]^n$
5	Set pbest[i] = position[i]
6	Compute fitness[i] = fitness(position[i])
7	END FOR
8	Set gbest = pbest[argmin(fitness)] and gbest_fitness = min(fitness)
9	Main Loop:
10	FOR t = 1 TO T DO:
11	Update inertia weight: $w = w_0 - (w_0 - w_{min})\frac{t}{T}$
12	Update transfer parameters:
13	$[\lambda(t) = \lambda_0 - (\lambda_0 - \lambda_{min})\frac{t}{T}]$
14	$[\delta(t) = \delta_0 + (\delta_{max} - \delta_0)\frac{t}{T}]$
15	Compute swarm mean: $[m = \frac{1}{N}\sum_{i=1}^{N} \text{position}[i]]$ for i = 1 to N
16	FOR i = 1 TO N DO:
17	Generate random vectors r1 and r2 (each dimension ∈ [0,1])
18	Update velocity[i]:
19	Eq. 25.
20	Update position[i]:
21	position[i] = CLIP(position[i] + velocity[i], 0, 1)
22	IF fitness(position[i]) < fitness(pbest[i]) THEN:
23	pbest[i] = position[i]
24	END IF
25	END FOR
26	Update gbest:
27	gbest = pbest[argmin(fitness(pbest))]
28	gbest_fitness = min(fitness(pbest))
29	FOR i = 1 TO N DO:
30	FOR each dimension j = 1 TO n DO:
31	Compute probability $[p = \frac{1}{1+\exp(-\lambda \cdot (\text{velocity}[i][j]-\delta))}]$
32	Set position[i][j] = 1 if random() < p, ELSE 0
33	END FOR
34	END FOR
35	END FOR
36	Return gbest and gbest_fitness
37	END.

While effective for certain binary optimization problems, the original AQBPSO may struggle in highly dynamic or complex landscapes—such as those encountered in 6 G IoT energy and resource allocation—due to its fixed mapping and standard velocity dynamics.

3.5.1. Proposed EAQBPSO

To address these challenges, we have introduced several modifications to create a more robust and adaptive algorithm:

Dynamic Inertia Weight $w(t)$: Rather than a fixed inertia weight, our version employs a linearly decreasing inertia weight, as defined by Eq. (23):

$$w(t) = w_0 - (w_0 - w_{min})\frac{t}{T} \tag{23}$$

Where w_0 and w_{min} are the initial and minimum weights, respectively. This allows the algorithm to emphasize exploration early on and shift toward exploitation as convergence nears.

Time-Varying Transfer Function Parameters ($\lambda(t)$and $\delta(t)$): We modify the standard sigmoid transfer function by introducing parameters that change over time, as calculated in Eq. (24):

$$T(v) = \frac{1}{1 + \exp(-\lambda(t)(v - \delta(t)))} \tag{24}$$

Here, $\lambda(t)$ (the slope) and $\delta(t)$ (the threshold shift) are updated iteratively, allowing the mapping from continuous positions to binary decisions to adapt based on the search progress.

Swarm Mean Guidance in Velocity Update: In addition to the classical PSO terms (personal best and global best differences), we incorporate an extra term that pulls each particle toward the mean position of the swarm, as shown in Eq. (25):

$$v_{i,j}(t+1) = w(t)v_{i,j}(t) + c_1 r_1\left(pbest_{i,j} - x_{i,j}(t)\right) + c_2 r_2\left(gbest_j - x_{i,j}(t)\right) + c_3\left(m_j(t) - x_{i,j}(t)\right) \tag{25}$$

where $m_j(t)$ is the mean position in the jth dimension, and c_3 is a coefficient controlling this term's influence. This collective guidance helps steer the particles toward promising regions, enhancing global convergence.

Enhanced Exploration via Quantum-Inspired Probabilistic Update: The adaptive transfer function provides a probabilistic "tunneling" effect. Even when particles are near local optima, the dynamic mapping allows them a controlled chance to flip states, improving the ability to escape local minima.

Algorithm 1 outline our propose EAQBPSO, which is designed to solve the NP-hard task scheduling and energy optimization problem in 6G-enabled batteryless IoT networks. In this algorithm, the population first initialized with random continuous positions and velocities. Each particle's personal best (pbest) and the global best (gbest) are compute based on the defined fitness function. The algorithm then enter a main loop where it dynamically update the inertia weight, following a linearly decreasing schedule (Eq. (23)), and adapts the transfer function parameters λ(t) and δ(t) over time (Eq. (24)). A swarm mean guidance term (Eq. (25)) is incorporate into the velocity update to steer particles toward promising regions in the search space. Finally, a quantum-inspired probabilistic

Table 3
Simulation Parameters.

Category	Parameter	Value
Network Model	Architecture	6G-enabled batteryless IoT with Vortex WPT and fog nodes
	Number of IoT Devices (N)	50 to 250
	Number of WPT Zones (Z)	Multiple vortex power transfer zones
	Number of Fog Nodes (M)	Multiple MEC fog nodes
Task Model	Tasks per Device	5 tasks per run
	Task Size Range	500 to 5000 units
Processing Model	Local Processing Frequency	1.2 GHz
	Offloading Processing Frequency	2.5 GHz
	Local Energy Consumption	2.5 energy units
	Offloaded Task Energy Consumption	1.0 energy units
	Overhead Energy	50 energy units
	Overhead Latency	0.1 s
WPT Model	Transmitted Power (Pwpt)	10,000 units
	Attenuation Reference Distance (d0)	10 units
	Efficiency (η)	0.8
	Maximum WPT Range (Rmax)	50 units
	Coverage Model	Distance-based power allocation
Energy Model	Power Demand Model	αd (1 + βd sin(ωt))
	Received Power Model	Precv(d,i,t) = ηi Pwpt exp(-λ rd,i)
	Energy Consumption Model	Econs(d) = Pd Top + Ptx Ttx
	Sustainability Constraint	Erecv(d) ≥ Econs(d)
Computation Offloading	Communication Model	6 G mmWave / THz bands
	Path Loss Model	Log-distance path loss with shadowing
	Offloading Decision Criteria	Based on energy, fog load, and link quality
Implementation	Programming Language	Python

binary updates is apply to convert the continuous positions into binary decisions. This procedure is repeated for a set number of epochs, and the algorithm returns the best solution and its fitness, effectively balancing exploration and exploitation while escaping local optima.

4. Simulation setup and parameters

Our simulation framework model a 6G-enabled batteryless IoT network with Vortex WPT and computation offloading to fog nodes, where N batteryless IoT devices dynamically switch between multiple WPT zones for energy harvesting and offload tasks to M fog nodes over 6 G mmWave THz links to meet energy and latency constraints. Each device generate five tasks per run, with task sizes range from 500 to 5000 units, and execute them either locally at 1.2 GHz with an energy consumption of 2.5 units per task or offloading them to fog nodes at 2.5 GHz, consuming 1.0 energy unit per task, with an additional 50 energy units and 0.1 s of overhead. The Vortex WPT system transmitted power at 10,000 units with an attenuation reference distance $(d0)$ of 10, efficiency (η) of 0.8, and maximum range of 50 units, where the power receive by each device follows received power based on its distance from the WPT center. The deployment spans a 100×100 unit area, accommodating 50 to 250 IoT devices, multiple Vortex WPT zones, and MEC-enabled fog nodes, with fog nodes constrained by a processing capacity (Cf) and a latency threshold (τf). To optimize task scheduling and energy-efficient offloading, we implemented four advanced metaheuristic algorithms: Adaptive Memetic Swarm Optimizer (AMSO) with a population size of 50 and 100 epochs, Hybrid Evolutionary-Swarm Annealing (HESA) and Adaptive Hybrid Evolutionary Swarm (AHES) both with population sizes of 30 and 100 epochs, and EAQBPSO with a population size of 30, 100 epochs, and an adaptive learning coefficient ($c3 = 1.0$), while a baseline random offloading strategy is used for comparison. The performance is evaluated using key metrics including energy efficiency, energy harvesting efficiency, device sustainability ratio, average energy consumption per task, fog node utilization ratio, sustainability margin, and resource allocation fairness, providing a comprehensive assessment of energy harvesting, offloading efficiency, and fog resource management in a 6G-enabled batteryless IoT network with Vortex WPT. Table 3 summarizes the simulation parameters and their values.

4.1. Comparison algorithms

To evaluate the effectiveness of the proposed EAQBPSO algorithm, we compare it against several state-of-the-art optimization techniques. These algorithms incorporate diverse optimization strategies, including swarm intelligence, evolutionary computation, and hybrid metaheuristics, each offering distinct advantages in terms of convergence speed, search efficiency, and adaptability to dynamic environments.

4.1.1. Adaptive memetic swarm optimizer (AMSO)

AMSO is a hybrid algorithm that combine the global search power of swarm intelligence with local search refinements drawn from memetic algorithms. It starts with a population of candidate solutions (as in PSO) and, at periodic intervals, applies a local search operator (for example, a simple bit-flip or gradient-based search) to the best-performing individuals. Key features of this algorithm are as follow:

Memetic Local Search: After each iteration or every few generations, the algorithm refines a subset of solutions with a dedicated local search, enabling faster convergence toward high-quality optima.

Adaptive Parameter Tuning: The inertia weight and acceleration coefficients are tuned over time based on the diversity and convergence behavior of the swarm.

Swarm Dynamics: Standard PSO components (personal and global best updates) guide the search, while the additional local search ensures that the algorithm escapes shallow local optima.

4.1.2. Hybrid evolutionary-swarm annealing (HESA)

HESA integrate elements from evolutionary algorithms, swarm intelligence, and simulated annealing. It uses evolutionary operators (such as selection, crossover, and mutation) to maintain diversity, and swarm updates drive the global search. A simulated annealing component is added to allow occasional acceptance of suboptimal moves, which aid in escaping local optima. Key features of this algorithm are as follow:

Evolutionary Operators: Selection and crossover help to combine and recombine good solution features from different individuals, and mutation introduces controlled random variations.

Swarm-Based Learning: The collective intelligence of the swarm (similar to PSO) provides an efficient mechanism for global exploration.

Simulated Annealing Phase: The annealing schedule, with a gradually decreasing temperature, probabilistically accepts worse solutions early on, thus allowing the algorithm to overcome local traps and converge toward a global optimum.

4.1.3. Adaptive hybrid evolutionary swarm (AHES)

AHES is a comprehensive hybrid algorithm that synergistically combines genetic algorithms (GA) and PSO with additional local search heuristics. This integration is performed adaptively so that the algorithm dynamically adjusts its strategies based on the current state of the search process. Key features of this algorithm are as follow:

Genetic Diversity: A GA-based method (with operators such as selection, crossover, and mutation) generate a diverse initial population and maintains global diversity throughout the search.

Swarm Intelligence: PSO-like update quickly guides the population toward promising regions in the search space by leveraging both personal best and global best positions.

Local Refinement: Periodic local search is applied to refine elite solutions, ensuring that local optima are efficiently exploited.

Adaptive Strategy: Parameters such as mutation rate, inertia weight, and crossover probability are adjusted on the fly based on convergence metrics, ensuring a balance between exploration and exploitation across iterations.

5. Simulation results and discussion

To assess the performance of our proposed model and the EAQBPSO algorithm, we define a series of metrics that capture various aspects of energy efficiency, sustainability, and resource allocation fairness in the network.

5.1. Energy efficiency (EE)

EE quantifies how effectively the harvested energy supports the operations of IoT devices. For each device, we compute the ratio of the average harvested energy E_{recv} to its total energy consumption E_{cons} over all its tasks. Mathematically, the EE metric is given by Eq. (26):

$$\text{EE} = \frac{1}{N}\sum_{d\in\mathscr{D}}\frac{E_{\text{recv},d}}{E_{\text{cons},d}} \tag{26}$$

where the harvested energy for a task is computed as Eq. (27):

$$E_{\text{recv}} = \eta P_{\text{wpt}} \exp\left(-\frac{d}{d_0}\right) \tag{27}$$

with d being a distance randomly sampled from a uniform distribution over the range $[0, R_{max}]$. A higher EE indicates that a greater proportion of consumed energy is replenished via WPT.

As shown in Fig. 4, for a large-scale setup with 250 IoT devices, the EAQBPSO algorithm show better energy efficency, clearly outpreforming other methods. EAQBPSO reach ~71 % improvement over Random, ~33 % over AMSO, ~50 % over AHES, and ~32 % over HESA. These gains come from EAQBPSO's ability to balance workloads, assign resources dynamically, and cut unneeded energy-heavy tasks. On the other hand, Random scheduling has the lowest efficiency because it lacks smart task assignment, causing more power usage. AMSO do better but fails to keep efficiency as the system grow. AHES, even with its heuristic optimization, does not adapt well to higher loads. HESA performs at a mid-level but still lose to EAQBPSO due to its stactic resource allocation approach.

5.2. Energy harvesting efficiency (EHE)

The EHE metric assesses the overall performance of the WPT system by comparing the total energy harvested by all devices to the maximum possible energy available. It is defined as Eq. (28):

$$\text{EHE} = \frac{\sum_{d\in\mathscr{D}}\overline{E_{\text{recv},d}}}{N \cdot P_{\text{wpt}}} \tag{28}$$

For each task, if the offloading decision is taken (solution bit ≥ 0.5), the device is assumed to be in a favorable zone (distance sampled from $\left[0, \frac{R_{max}}{2}\right]$ *if* processed locally (solution bit < 0.5), a less favorable zone is assumed (distance sampled from $\left[\frac{R_{max}}{2}, R_{max}\right]$. The

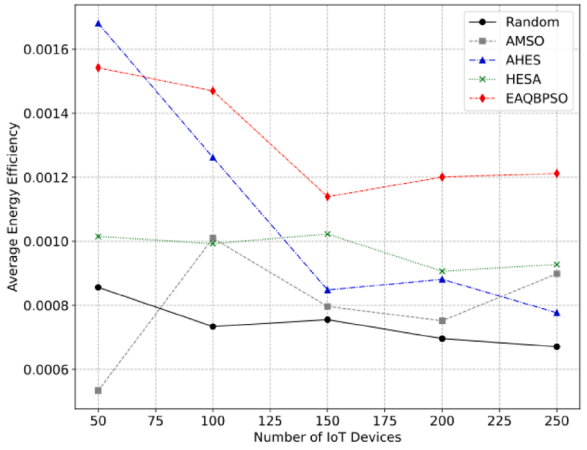

Fig. 4. Energy Efficiency Analysis Across Different Optimization Methods.

average harvested energy per device is then used to compute EHE.

Fig. 5 show how EAQBPSO affects EHE when running with 250 IoT devices, bringing signficant improvements over other methods. EAQBPSO reach 87.03 % more efficiency than Random and outperforms AMSO, AHES, and HESA by 48.51 %, 35.87 %, and 28.44 %, repectively. These gains come from EAQBPSO's smart energy management and scheduling, which optmize harvesting and allocation based on chaging workloads. Random scheduling lack control over resource use, while AMSO face issues with efficiency as system complexity grow. AHES uses heuristic optimization, but it fails to stay flexible with different task loads. HESA also performe moderately, but its static resource policies limits adaptability.

5.3. Average energy consumption per task (AECT)

AECT is a straightforward metric that captures the average energy consumption incurred for processing each task. It is calculated as Eq. (29):

$$\text{AECT} = \frac{\sum_{d \in \mathscr{D}} E_{\text{cons},d}}{\text{Total Number of Tasks}} \tag{29}$$

where $E_{\text{cons},d}$ is the energy consumed by device d for its tasks (using local energy if processed locally and offloading energy if offloaded). Lower values of AECT indicate a more energy-efficient operation across the network.

As shown in Fig. 6, for a case with 250 IoT devices, the EAQBPSO algorithm decrease AECT more than other methods. It reduces AECT by 40.80 % over Random, 30.38 % over AMSO, 21.73 % over AHES, and 21.97 % over HESA. These reductions prove that EAQBPSO optimize task execution while lowering unnecessary power use. Random scheduling uses the most energy since it lack workload balancing. AMSO performs better but fails to scale well under heavy taks loads. AHES and HESA work better, but their heuristic-based strategies are less effective in changing conditions, leading to less eficient energy use.

Fig. 7 and Table 4, Table 5, and Table 5 show the performance of EAQBPSO across different metrics. Table 3 highlights the superiror EE achieved by EAQBPSO, with a mean of 1.31E-03 and a standard devation of 1.61E-04, ensuring better efficiency and stability. Compared to AHES, it rise the median EE by 3.30E-04 while goes beyond HESA's maximum EE by 5.20E-04. Traditional methods like Random (7.42E-04) and the method AMSO (7.98E-04) show much lower performance, proving the effectiveness of EAQBPSO.

Table 4 also prove the advantages in EHE, where EAQBPSO reach a mean of 2.89E-01 with small variation (std. 4.39E-03). It surpasses AHES by 4.40E-02 in mean EHE and overcome HESA's median by 5.20E-02, showing strong efficiency gains. In contrast, AMSO (2.10E-01) and Random (1.57E-01) stay behind, highlighting EAQBPSO's adaptive resource use.

Table 5 showcase EAQBPSO's ability to reduce energy consumption, with an average AECT of 2.88E+03, the lowest among all methods. It cut median AECT by 6.40E+02 compared to AMSO and also 6.40E+02 lower than AHES. The model achieves a 41.62 % lower maximum AECT than Random, strengthening its role in efficient energy management. These results together prove EAQBPSO's superiority in balancing energy efficiency, harvesting power, and lowering consumption, making it a strong solution for the proposed environment.

5.4. Device sustainability ratio

The Device Sustainability Ratio (DSR) measures the proportion of IoT devices that are able to harvest enough energy to meet their operational consumption. For each device, we sum its energy consumption and harvested energy over all tasks, then define the device as sustainable if

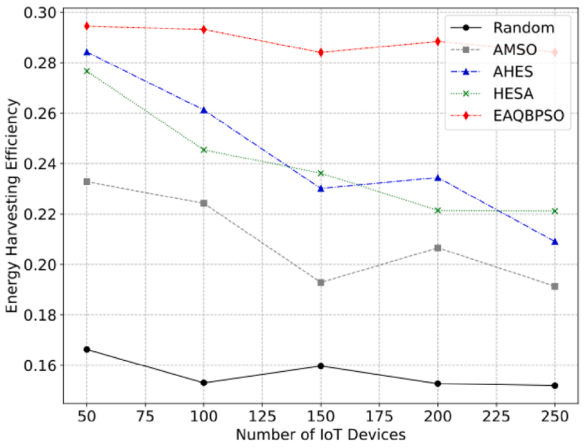

Fig. 5. Comparative Analysis of Energy Harvesting Efficiency in IoT Networks Across Different Optimization Methods.

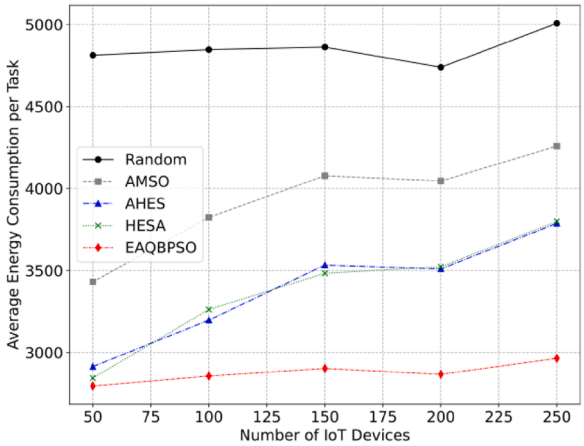

Fig. 6. Impact of Optimization Strategies on Task Energy Consumption.

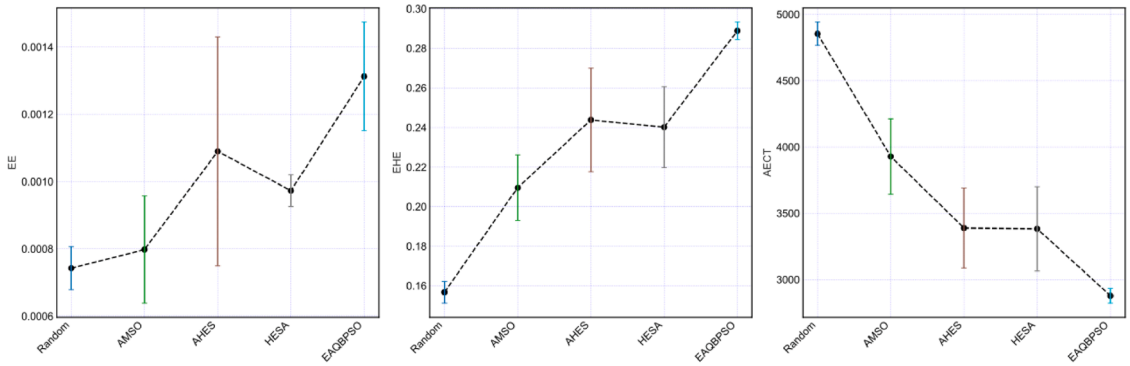

Fig. 7. Comparative Analysis of EE, EHE, and AECT Across Optimization Methods.

Table 4
The statistical analysis of EE for the algorithms.

Method	Min	Max	Mean	50 %	Std.
Random	6.71E-04	8.56E-04	7.42E-04	7.34E-04	6.40E-05
AMSO	5.34E-04	1.01E-03	7.98E-04	7.96E-04	1.59E-04
AHES	7.77E-04	1.68E-03	1.09E-03	8.81E-04	3.40E-04
HESA	9.07E-04	1.02E-03	9.73E-04	9.93E-04	4.71E-05
EAQBPSO	1.14E-03	1.54E-03	1.31E-03	1.21E-03	1.61E-04

Table 5
The statistical analysis of EHE for the algorithms.

Method	Min	Max	Mean	50 %	Std.
Random	1.52E-01	1.66E-01	1.57E-01	1.53E-01	5.50E-03
AMSO	1.91E-01	2.33E-01	2.10E-01	2.07E-01	1.66E-02
AHES	2.09E-01	2.84E-01	2.44E-01	2.34E-01	2.62E-02
HESA	2.21E-01	2.77E-01	2.40E-01	2.36E-01	2.04E-02
EAQBPSO	2.84E-01	2.95E-01	2.89E-01	2.88E-01	4.39E-03

$$E_{\text{recv},d} \geq E_{\text{cons},d} \tag{30}$$

Thus, DSR is given by Eq. (31):

$$\text{DSR} = \frac{\left\{d \in \mathscr{D} : E_{\text{recv},d} \geq E_{\text{cons},d}\right\}}{N} \tag{31}$$

In our simulation, when a task is processed locally (solution bit < 0.5), the distance d is sampled from $[0.6 \times R_{max}, 0.9 \times R_{max}]$; when offloaded (solution bit ≥ 0.5), d is sampled from $[0.1 \times R_{max}, 0.4 \times R_{max}]$.

The results in Fig. 8 show how EAQBPSO affects device sustainability ratio (DSR) in a network with 250 IoT devices. EAQBPSO gets a 27.55 % improvement over Random, 6.84 % over AMSO, 2.46 % over AHES, and 2.04 % over HESA. This proves its ability to increase device longevity and reliability. Random scheduling has low sustainability because of bad task distribution. AMSO performs beter but fail to optimize resource usage when workload grow. AHES and HESA keep high DSR values, but EAQBPSO outpreforms them with adaptive workload balancing and energy-aware scheduling.

5.5. Sustainability margin

The Sustainability Margin (SM) provides a relative measure of energy surplus (or deficit) at each device. For each device d, the margin is defined as Eq. (32):

$$M_d = \frac{E_{\text{recv},d} - E_{\text{cons},d}}{E_{\text{cons},d}} \tag{32}$$

and the network-wide SM is the average margin across devices, as given by Eq. (33):

$$\text{SM} = \frac{1}{N} \sum_{d \in \mathcal{D}} M_d \tag{33}$$

A positive SM shows that devices on average use more energy than they consume.

Fig. 9 shows the performance of EAQBPSO for SM when used with 250 IoT devices. Compare to other methods, EAQBPSO increase performance by 138.55 % over Random method, 74.10 % over AMSO, 37.62 % over AHES, and 44.09 % over HESA. This difference in results prove that EAQBPSO keep the system stable under high computational demmand. While Random scheduling have trouble with task execution, AMSO make some improvements but lack adaptability for larger workloads. AHES and HESA, though somewhat beter, still cannot reach the optimization level of EAQBPSO.

5.6. Fog node utilization ratio (FNUR)

FNUR measures the extent to which the available computational capacity of the fog nodes is utilized by offloaded tasks. Assuming that each offloaded task contributes a load proportional to its task size (multiplied by a factor), the total offloaded load is defined as Eq. (34):

$$\text{Load} = \sum_{\text{offloaded tasks}} (\text{task size} \times \text{factor}) \tag{34}$$

and FNUR is given by Eq. (35):

$$\text{FNUR} = \frac{\text{Total Offloaded Load}}{M \cdot C_f} \tag{35}$$

where M is the number of fog nodes and C_f is the capacity per fog node. A higher FNUR indicates greater utilization of the fog nodes relative to their available capacity.

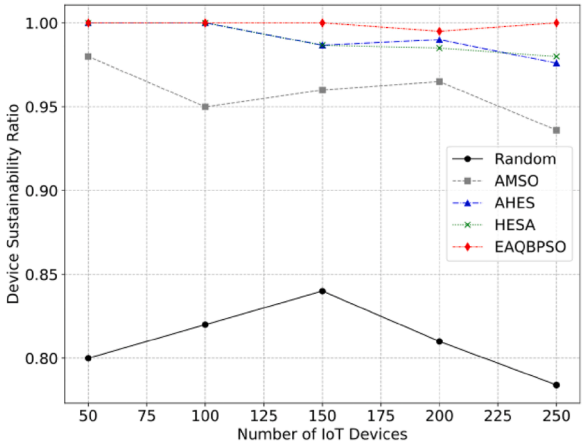

Fig. 8. Impact of Optimization Strategies on Device Sustainability Ratio.

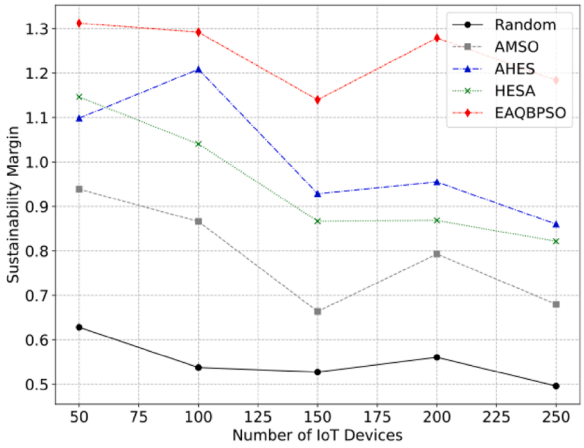

Fig. 9. Impact of Optimization Strategies on Sustainability Margin.

An analysis of FNUR for a setup with 250 IoT devices, as shown in Fig. 10, reveal the optmized performance of EAQBPSO compared to other methods. EAQBPSO boost FNUR by 98 % over Random scheduling, while surpassing AMSO by 44 %, AHES by 24 %, and HESA by 25 %. This improvment in FNUR indicate that EAQBPSO helps balance computational workloads better across fog nodes, reduce bottlenecks, and make resource usage more eficient.

An evaluation of DSR, SM, and FNUR for different algorithms is show in Fig. 11, Table 7, Table 8, and Table 9. The DSR results in Table 6 indicate that EAQBPSO keep optimal sustainability, with a mean of 9.99E-01 and a low standard devotion of 2.00E-03. This means it is more optimize than AMSO by 4.00E-02 and improves Random's performance by 24.07 %. For SM (Table 7), EAQBPSO gets a mean of 1.24E+00, surpassing other methods by a huge margin. Its median value is 1.28E+00, higher than AHES by 3.26E-01, and its maximum is optimized than HESA by 1.60E-01. This show that EAQBPSO improves long-term energy availability in systems with limited resources. Table 8 focus on FNUR, showing how EAQBPSO make resource usage better. The mean FNUR is 3.98E+00, which increase by 1.11E+00 compared to AMSO and by 6.00E-01 over AHES. The highest FNUR of 6.65E+00 under EAQBPSO shows more balancing and better resource allocation in fog nodes.

5.7. *Resource allocation fairness (RAF)*

RAF is computed using Jain's Fairness Index and quantifies how evenly the offloaded computational load is distributed among IoT devices. For each device d, let L_d denote the total offloaded load (calculated as the sum of task sizes multiplied by a load factor for offloaded tasks). RAF is then computed as Eq. (36):

$$\mathrm{RAF} = \frac{\left(\sum_{d\in\mathscr{D}} L_d\right)^2}{N \cdot \sum_{d\in\mathscr{D}} L_d^2} \tag{36}$$

A RAF value close to 1 indicates a fair distribution of resources, whereas lower values suggest an imbalance in resource allocation.

In evaluating RAF for a network with 250 IoT devices, as depicted in Fig. 12, it highlights EAQBPSO's ability to obtains more balanced resource distribution. The algorithm improve fairness by 23.32 % over Random, 11.03 % over AMSO, 5.20 % over AHES, and 6.69 % over HESA. These outcomes indicate that EAQBPSO effectively minimizes resource disparity among fog nodes, ensuring a more equitable tasks distribution. Random scheduling produce the lowest fairness, since it lacking an advanced assignment method, while AMSO moderately enhances fairness but do not fully optimize allocation efficiency at large scales. AHES and HESA shows improvements, yet their heuristic-driven strategies do not fully adapt to dynamic workload variations, causing inconsistent resource usage.

In the analysis of RAF shown in Table 10 and Fig. 13, EAQBPSO effectively demonstrate a more balanced task distribution across the system. With an average RAF of 9.49E-01 and a standard deviation of 4.03E-03, EAQBPSO not only maintains an equitable resource allocation but also preserves consistent performance. The algorithm significantly outperforms AHES by 3.60E-02 and HESA by 4.50E-02, underlining its capacity to reduce resource contention. Compared to AMSO, EAQBPSO attains a 9.85 % uptick in mean fairness, while exceeding Random's top RAF by 1.52E-01. This outcome further demonstrates the algorithm's advanced scheduling approach, as its median RAF (9.49E-01) surpass that of AMSO and HESA by 9.30E-02 and 5.70E-02, sustaining fairness under various workload. While Random scheduling struggles with inefficient task balancing, and AMSO only yields moderate gains, EAQBPSO employs adaptive scheduling mechanisms to minimize disparity. Moreover, the small standard deviation of 4.03E-03 highlight that EAQBPSO persistently upholds fairness, unlike heuristic-based solutions that often exhibit greater inconsistency.

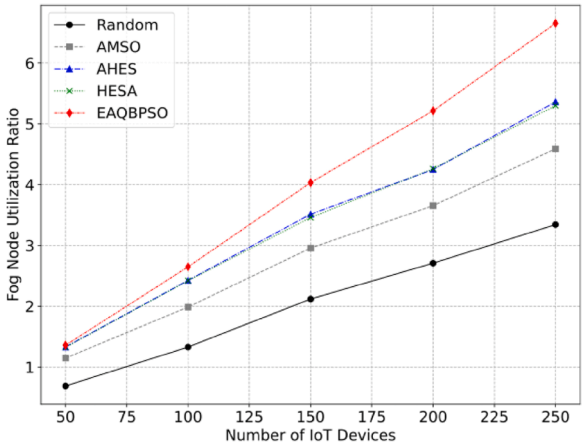

Fig. 10. Impact of Optimization Strategies on Fog Node Utilization Ratio.

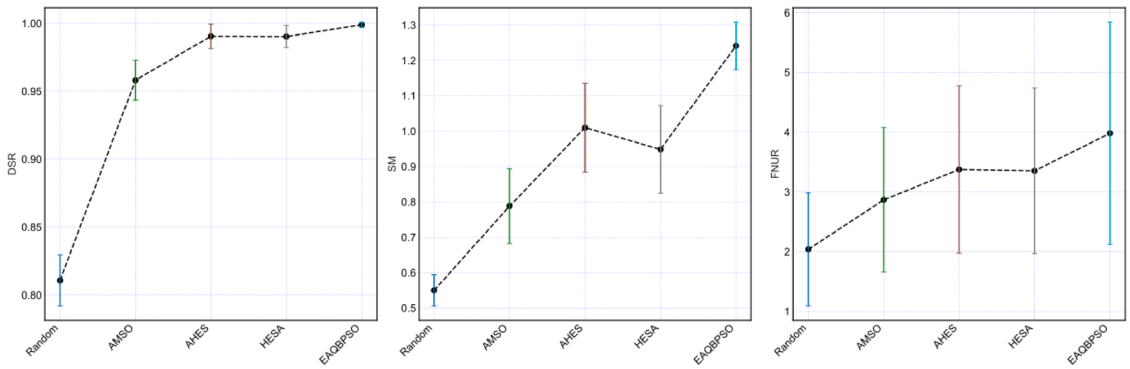

Fig. 11. Comparative Analysis of DSR, SM, and FNUR Across Optimization Methods.

Table 6
The statistical analysis of AECT for the algorithms.

Method	Min	Max	Mean	50 %	Std.
Random	4.74E+03	5.01E+03	4.85E+03	4.85E+03	8.78E+01
AMSO	3.43E+03	4.26E+03	3.93E+03	4.05E+03	2.84E+02
AHES	2.91E+03	3.79E+03	3.39E+03	3.51E+03	3.02E+02
HESA	2.84E+03	3.80E+03	3.38E+03	3.48E+03	3.18E+02
EAQBPSO	2.80E+03	2.96E+03	2.88E+03	2.87E+03	5.55E+01

Table 7
The statistical analysis of DSR for the algorithms.

Method	Min	Max	Mean	50 %	Std.
Random	7.84E-01	8.40E-01	8.11E-01	8.10E-01	1.88E-02
AMSO	9.36E-01	9.80E-01	9.58E-01	9.60E-01	1.47E-02
AHES	9.76E-01	1.00E+00	9.91E-01	9.90E-01	9.01E-03
HESA	9.80E-01	1.00E+00	9.90E-01	9.87E-01	8.19E-03
EAQBPSO	9.95E-01	1.00E+00	9.99E-01	1.00E+00	2.00E-03

5.8. Possible limitations and real-world deployment challenges

While the proposed model demonstrates strong performance in simulation, several technical challenges must be addressed for real-world deployment. First, the energy harvesting model relies on idealized vortex WPT propagation with exponential attenuation. However, physical environments often introduce non-idealities such as multipath fading, device orientation mismatch, and environmental obstacles (e.g., walls, vegetation), which degrade energy reception. These losses can severely impact the sustainability

Table 8
The statistical analysis of SM for the algorithms.

Method	Min	Max	Mean	50 %	Std.
Random	4.96E-01	6.28E-01	5.50E-01	5.38E-01	4.42E-02
AMSO	6.64E-01	9.39E-01	7.88E-01	7.93E-01	1.06E-01
AHES	8.60E-01	1.21E+00	1.01E+00	9.55E-01	1.26E-01
HESA	8.22E-01	1.15E+00	9.49E-01	8.68E-01	1.24E-01
EAQBPSO	1.14E+00	1.31E+00	1.24E+00	1.28E+00	6.73E-02

Table 9
The statistical analysis of FNUR for the algorithms.

Method	Min	Max	Mean	50 %	Std.
Random	6.89E-01	3.34E+00	2.04E+00	2.12E+00	9.47E-01
AMSO	1.15E+00	4.59E+00	2.87E+00	2.96E+00	1.21E+00
AHES	1.33E+00	5.36E+00	3.38E+00	3.51E+00	1.40E+00
HESA	1.33E+00	5.30E+00	3.35E+00	3.46E+00	1.39E+00
EAQBPSO	1.36E+00	6.65E+00	3.98E+00	4.03E+00	1.86E+00

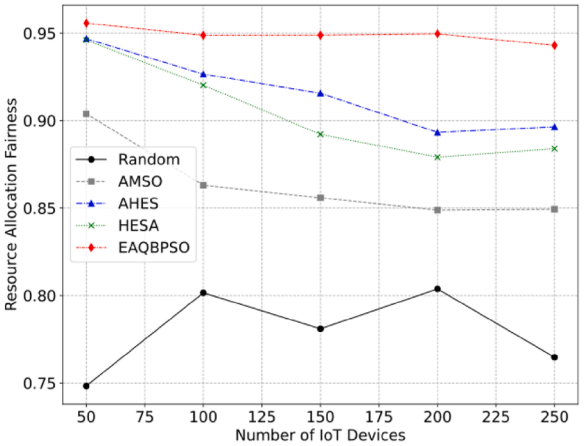

Fig. 12. Impact of Optimization Strategies on Resource Allocation Fairness.

Table 10
The statistical analysis of RAF for the algorithms.

Method	Min	Max	Mean	50 %	Std.
Random	7.48E-01	8.04E-01	7.80E-01	7.81E-01	2.13E-02
AMSO	8.49E-01	9.04E-01	8.64E-01	8.56E-01	2.05E-02
AHES	8.93E-01	9.47E-01	9.16E-01	9.16E-01	1.98E-02
HESA	8.79E-01	9.46E-01	9.04E-01	8.92E-01	2.53E-02
EAQBPSO	9.43E-01	9.56E-01	9.49E-01	9.49E-01	4.03E-03

guarantees observed in controlled simulations. Second, the framework assumes continuous knowledge of each IoT device's position, power consumption, and WPT zone coverage. In practice, real-time localization and energy state monitoring require additional sensors, energy meters, and communication overhead, which increase system complexity and drain limited harvested energy. Third, the fog layer is assumed to be always available with reliable 6 G connectivity. In reality, fog nodes may experience intermittent failures, resource contention, and backhaul delays, leading to task rejection or deadline violations for latency-critical applications. Fourth, although the EAQBPSO algorithm scales well in simulation, its computational burden (multiple particles, adaptive parameters, sigmoid transformations) may exceed the capabilities of low-power microcontrollers or fog agents, delaying convergence and reducing real-time adaptability. Fifth, vortex-based WPT at high frequencies (e.g., THz) faces unresolved regulatory, electromagnetic safety, and standardization issues. Public exposure limits and certification constraints may delay deployment. Finally, the model does not yet include secure authentication or jamming resilience mechanisms. Spoofing fog nodes or interfering with WPT signals could lead to malicious energy deprivation or incorrect task migration decisions.

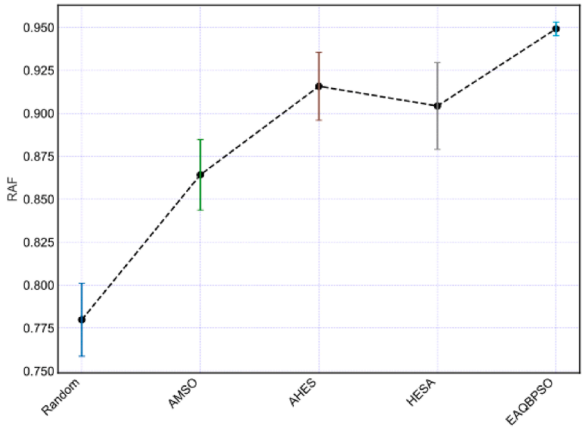

Fig. 13. Comparative Analysis of RAF Across Optimization Methods.

6. Conclusion and future works

In this paper, we introduce an energy-driven model for a 6G-supported batteryless IoT network that utilize WPT and fog coordination to flexibly manage energy harvesting and computation offloading. Our experimental results are showing that the proposed EAQBPSO approach generally surpass other methods—boosting energy efficiency by up to 71 %, enhancing energy harvesting by nearly 87 %, lowering AECT by over 40 %, and delivering near-optimal device sustainability as well as fair resource allocation. Despite such achievements, our research encounter several limitations. Foremost, the simulation platform depends on simulation parameters and energy models that may not fully capturing the variability in real-world settings, nor does it cover potential security vulnerabilities such as signal jamming or unauthorized access, which might undermine energy distribution and offloading decisions. Secondly, the computational demands of the hybrid metaheuristics may hinder scalability in extremely large networks, and the current framework lacks security protections during distributed processing. Third, even if the model reveals significant performance gains, its responsiveness to highly dynamic network situations and emergent security hazards remains unresolved. Future extensions will explore scalability under heterogeneous and mobile conditions, incorporating adaptive scheduling and fog-cloud coordination to maintain performance across dynamic topologies, device mobility, and varying energy profiles in large-scale batteryless IoT environments, and should concentrate on incorporating real-world data for validation, devising adaptive and real-time optimization strategies with integrated security measures, and exploring optimization approaches to further fortify both the performance and security of batteryless IoT networks in 6 G contexts.

Declarations

Ethical Approval: The authors of this paper declare that they have entirely avoided publishing ethics, including plagiarism, misconduct, falsification of data, or double submission and publication, regarding the publication of the presented article. There is no commercial in this regard, and the authors have not received any money for presenting their paper. The corresponding author also declares that this paper has not been published elsewhere and has yet to be submitted to another publication simultaneously.

CRediT authorship contribution statement

Mehdi Hosseinzadeh: Writing – original draft, Conceptualization. **Jawad Tanveer:** Writing – review & editing, Data curation. **Saqib Ali:** Writing – review & editing, Resources, Conceptualization. **Marcia L. Baptista:** Methodology, Visualization, Writing – review & editing. **Farhad Soleimanian Gharehchopogh:** Writing – original draft, Methodology, Conceptualization. **Shakia Rajabi:** Writing – original draft, Methodology, Conceptualization. **Thantrira Porntaveetus:** Writing – review & editing, Resources, Data curation. **Sang-Woong Lee:** Writing – review & editing, Methodology, Data curation.

Declaration of competing interest

The authors declare that they have no known competing financial interests or personal relationships that could have appeared to influence the work reported in this paper.

Acknowledgment

This work was supported by national funds through FCT (Fundação para a Ciência e a Tecnologia), under the project - UIDB/04152 - Centro de Investigação em Gestão de Informação (MagIC)/NOVA IMS.

Data availability

No data was used for the research described in the article.

References

[1] G. Moloudian, et al., RF energy harvesting techniques for battery-less wireless sensing, industry 4.0, and Internet of Things: a review, IEEE Sens. J. 24 (5) (2024) 5732–5745, https://doi.org/10.1109/JSEN.2024.3352402.

[2] S. Ullah, et al., A survey on emerging trends and applications of 5G and 6G to healthcare environments, ACM Comput. Surv 57 (4) (2024), https://doi.org/10.1145/3703154. Article 85.

[3] D.C. Nguyen, et al., 6G Internet of Things: a comprehensive survey, IEEE Internet Things J. 9 (1) (2022) 359–383, https://doi.org/10.1109/JIOT.2021.3103320.

[4] H. Nguyen, I. Al, Y.M. Jang, Survey of next-generation optical wireless communication technologies for 6G and beyond 6G, ICT Express (2025), https://doi.org/10.1016/j.icte.2025.04.006, 2025/04/15/.

[5] A. Alabsi, et al., Wireless power transfer technologies, applications, and future trends: a review, IEEE Trans. Sustain. Comput. 10 (1) (2025) 1–17, https://doi.org/10.1109/TSUSC.2024.3380607.

[6] Y. Zheng, et al., Wireless laser power transmission: recent progress and future challenges, Space Sol. Power Wirel. Transm. 1 (1) (2024) 17–26, https://doi.org/10.1016/j.sspwt.2023.12.001, 2024/06/01/.

[7] W. Liu, K.T. Chau, X. Tian, H. Wang, Z. Hua, Smart wireless power transfer — Opportunities and challenges, Renew. Sustain. Energy Rev. 180 (2023) 113298, https://doi.org/10.1016/j.rser.2023.113298, 2023/07/01/.

[8] M.A. Ullah, R. Keshavarz, M. Abolhasan, J. Lipman, K.P. Esselle, N. Shariati, A review on antenna technologies for ambient RF energy harvesting and wireless power transfer: designs, challenges and applications, IEEE Access 10 (2022) 17231–17267, https://doi.org/10.1109/ACCESS.2022.3149276.

[9] G.K. Ijemaru, K.L.-M. Ang, J.K. Seng, Wireless power transfer and energy harvesting in distributed sensor networks: survey, opportunities, and challenges, Int. j. distrib. sens. netw. 18 (3) (2022) 15501477211067740.

[10] A. Hazra, P. Rana, M. Adhikari, T. Amgoth, Fog computing for next-generation Internet of Things: fundamental, state-of-the-art and research challenges, Comput. Sci. Rev. 48 (2023) 100549, https://doi.org/10.1016/j.cosrev.2023.100549, 2023/05/01/.

[11] M.H. Alsharif, et al., Survey of energy-efficient fog computing: techniques and recent advances, Energy Rep. 13 (2025) 1739–1763, https://doi.org/10.1016/j.egyr.2025.01.039, 2025/06/01/.

[12] R. Das, M.M. Inuwa, A review on fog computing: issues, characteristics, challenges, and potential applications, Telemat. Inform. Rep. 10 (2023) 100049, https://doi.org/10.1016/j.teler.2023.100049, 2023/06/01/.

[13] A.M. Rahmani, et al., Self-learning adaptive power management scheme for energy-efficient IoT-MEC systems using soft actor-critic algorithm, Internet Things 31 (2025) 101587, https://doi.org/10.1016/j.iot.2025.101587, 2025/05/01/.

[14] K. Moghaddasi, S. Rajabi, F.S. Gharehchopogh, A. Ghaffari, An advanced deep reinforcement learning algorithm for three-layer D2D-edge-cloud computing architecture for efficient task offloading in the Internet of Things, Sustain. Comput.: Inform. Syst. 43 (2024) 100992, https://doi.org/10.1016/j.suscom.2024.100992, 2024/09/01/.

[15] U.M. Malik, M.A. Javed, S. Zeadally, S.u. Islam, Energy-efficient fog computing for 6G-enabled massive IoT: recent trends and future opportunities, IEEE Internet Things J. 9 (16) (2022) 14572–14594, https://doi.org/10.1109/JIOT.2021.3068056.

[16] P. Pandiyan, S. Saravanan, R. Kannadasan, S. Krishnaveni, M.H. Alsharif, M.-K. Kim, A comprehensive review of advancements in green IoT for smart grids: paving the path to sustainability, Energy Rep. 11 (2024) 5504–5531, https://doi.org/10.1016/j.egyr.2024.05.021, 2024/06/01/.

[17] A.M. Nemati, N. Mansouri, Resource allocation in fog computing: a survey on current state and research challenges, Knowl. Inf. Syst. 67 (3) (2025) 2091–2170, https://doi.org/10.1007/s10115-024-02274-5, 2025/03/01.

[18] S. Zhang, et al., Blockchain and federated deep reinforcement learning based secure cloud-edge-end collaboration in power IoT, IEEE Wirel. Commun. 29 (2) (2022) 84–91, https://doi.org/10.1109/MWC.010.2100491.

[19] N. Agrawal, A. Bansal, K. Singh, C.P. Li, S. Mumtaz, Finite block length analysis of RIS-assisted UAV-based multiuser IoT communication system with non-linear EH, IEEE Trans. Commun. 70 (5) (2022) 3542–3557, https://doi.org/10.1109/TCOMM.2022.3162249.

[20] A. Sabovic, A.K. Sultania, C. Delgado, L.D. Roeck, J. Famaey, An energy-aware task scheduler for energy-harvesting batteryless IoT devices, IEEE Internet Things J. 9 (22) (2022) 23097–23114, https://doi.org/10.1109/JIOT.2022.3185321.

[21] C. Delgado, J. Famaey, Optimal energy-aware task scheduling for batteryless IoT devices, IEEE Trans. Emerg. Top. Comput. 10 (3) (2022) 1374–1387, https://doi.org/10.1109/TETC.2021.3086144.

[22] A. Sabovic, M. Aernouts, D. Subotic, J. Fontaine, E. De Poorter, J. Famaey, Towards energy-aware tinyML on battery-less IoT devices, Internet Things 22 (2023) 100736, https://doi.org/10.1016/j.iot.2023.100736, 2023/07/01/.

[23] C.-C. Yang, R. Pandey, T.-Y. Tu, Y.-P. Cheng, P.C.P. Chao, An efficient energy harvesting circuit for batteryless IoT devices, Microsyst. Technol. 26 (1) (2020) 195–207, https://doi.org/10.1007/s00542-019-04544-7, 2020/01/01.

[24] P.C.d. Lacerda, A.A. Mariano, G. Brante, O.L.A. López, K. Mikhaylov, R.D. Souza, Behavioral modeling of a radio frequency wireless power transfer system for batteryless internet of things applications, IEEE Access 12 (2024) 86974–86984, https://doi.org/10.1109/ACCESS.2024.3416702.

[25] Y. Tang, G. Yin, P. Cong, J. Sun, J. Zhou, A discrete grey wolf optimizer metaheuristic for task offloading in multi-server MEC with batteryless devices, in: 2023 IEEE 29th International Conference on Parallel and Distributed Systems (ICPADS) 2023, 2023, pp. 2235–2242, https://doi.org/10.1109/ICPADS60453.2023.00301, 17-21 Dec.

[26] Z. Wang, et al., An energy-efficient all-dynamic multiparameter sensor for battery-less smart nodes in agricultural internet-of-things, IEEE Sens. J. 24 (13) (2024) 21426–21435, https://doi.org/10.1109/JSEN.2024.3396842.

[27] M. Bolourian, H. Shah-Mansouri, Energy-efficient task offloading for three-tier wireless-powered mobile-edge computing, IEEE Internet Things J. 10 (12) (2023) 10400–10412, https://doi.org/10.1109/JIOT.2023.3238329.

[28] D.V. Leemput, J. Hoebeke, E.D. Poorter, Integrating battery-less energy harvesting devices in Multi-hop Industrial wireless sensor networks, IEEE Commun. Mag. 62 (7) (2024) 66–73, https://doi.org/10.1109/MCOM.001.2300586.

[29] P.P. Puluckul, R.K. Singh, M. Weyn, TEGBed: a thermal energy harvesting testbed for batteryless internet of things, Internet Things 25 (2024) 101060, https://doi.org/10.1016/j.iot.2024.101060, 2024/04/01/.

[30] X. Fan, J. Hu, K. Yang, Martingale theory based definition and analysis of energy self-sustainability in batteryless internet of things, IEEE Trans. Green Commun. Netw. (2024) 1, https://doi.org/10.1109/TGCN.2024.3465877.